Inorganic Chemistry

Article

pubs.acs.org/IC

Influence of the Substituents on the Electronic and Electrochemical Properties of a New Square-Planar Nickel-Bis(quinoxaline-6,7-dithiolate) System: Synthesis, Spectroscopy, Electrochemistry, Crystallography, and Theoretical Investigation†

Ramababu Bolligarla, Samala Nagaprasad Reddy, Gummadi Durgaprasad, Vudagandla Sreenivasulu, and Samar K. Das*

School of Chemistry, University of Hyderabad, P.O. Central University, Hyderabad 500046, India

Supporting Information

ABSTRACT: We describe the synthesis, crystal structures, electronic absorption spectra, and electrochemistry of a series of square-planar nickel-bis(quinoxaline-6,7-dithiolate) complexes with the general formula $[Bu_4N]_2[Ni(X_2 6,7\text{-qdt})_2]$, where X = H (**1a**), Ph (**2a**), Cl (**3**), and Me (**4**). The solution and solid-state electronic absorption spectral behavior and electrochemical properties of these compounds are strongly dependent on the electron donating/accepting nature of the substituent X, attached to the quinoxaline-6,7-dithiolate ring in the system $[Bu_4N]_2[Ni(X_2 6,7\text{-qdt})_2]$. Particularly, the charge transfer (CT) transition bands observed in the visible region are greatly affected by the electronic nature of the substituent. A possible explanation for this influence of the substituents on electronic absorption and electrochemistry is described based on highest occupied molecular orbital (HOMO) to lowest unoccupied molecular orbital (LUMO) gaps, which is further supported by ground-state electronic structure calculations. In addition to this, the observed CT bands in all the complexes are sensitive to the solvent polarity. Interestingly, compounds **1a**, **2a**, **3**, and **4** undergo reversible oxidation at very low oxidation potentials appearing at $E_{1/2}$ = +0.12 V, 0.033 V, 0.18 V, and 0.044 V vs Ag/AgCl, respectively, in MeOH solutions, corresponding to the respective couples $[Ni(X_2 6,7\text{-qdt})_2]^-/[Ni(X_2 6,7\text{-qdt})_2]^{2-}$. Compounds **1a**, **3**, and **4** have been characterized unambiguously by single crystal X-ray structural analysis; compound **2a** could not be characterized by single crystal X-ray structure determination because of the poor quality of the concerned crystals. Thus, we have synthesized the tetraphenyl phosphonium salt of the complex anion of **2a**, $[PPh_4]_2[Ni(Ph_2 6,7\text{-qdt})_2]\cdot 3DMF$ (**2b**) for its structural characterization.

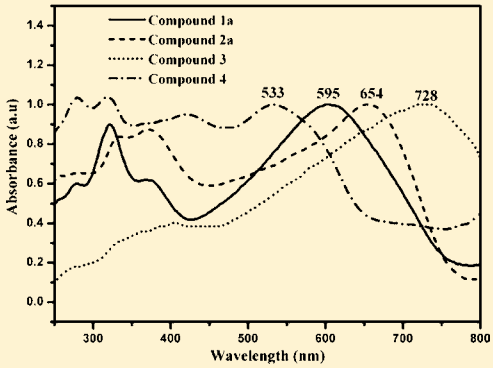

INTRODUCTION

Metal-dithiolene complexes have been of considerable interest to inorganic chemists for more than four decades because of their unique properties, and they provide redox active ligands with the ability to form highly electron-delocalized complexes.[1] The increasing attention in the design and synthesis of metal−dithiolene complexes is due to their potential applications in the areas of conducting-, magnetic-,[2] nonlinear optical-materials[3] and near-infrared (NIR) dyes.[4] The recent interest in metal dithiolene complexes in the area of bioinorganic modeling studies is due to the existence of a metal−dithiolene moiety in the active sites of many metallo-enzymes (hydroxylase-type molybdo-enzymes).[5,6] This metal-dithiolene containing active site has been characterized as "molybdopterin" (cofactor of the relevant metalloenzyme). The molybdopterin is basically a nitrogen atom containing heterocyclic based dithiolato-metal-oxo complex. Thus quinoxaline-2,3-dithiolate (qdt^{2-}, Scheme 1) and its molybdenum-oxo complexes have been investigated extensively for modeling the active sites of molybdenum hydroxylase enzymes.[7] Besides its biological relevance, qdt^{2-} ligand plays an important role in materials synthesis. This is because heterocyclic based dithiolene systems containing N and S atoms offer secondary coordination in addition to dithiolate coordination.[8] To achieve such materials, synthetic chemists have designed and synthesized diverse dithiolene ligands with nitrogen coordinating groups of increasing complexity.[9] We are particularly interested in synthesizing a qdt-based system because of its use in diverse areas. For example, qdt-based systems have been used in the development of field-effect transistors by introducing the fused qdt-based systems to the TTF-skeleton.[10] The photophysical (luminescence) properties of platinum complexes of qdt-type ligand have been studied extensively by Eisenberg's group.[11] McMaster, Garner, Kirk, and their co-workers reported the first example of valence tautomerism in a Mo-complex, which is nothing but a qdt-ligated molybdenum complex anion $[MoO(qdt)_2]^-$.[12] We studied the acid−base properties of nickel- and platinum-qdt system including their spectral properties.[13] Recently, we have reported the new quinoxaline

Received: May 16, 2012
Published: December 10, 2012

   dx.doi.org/10.1021/ic301017g | Inorg. Chem. 2013, 52, 66−76

Scheme 1. (a) Structural Representation of Quinoxaline Dithiolate Ligands; (b) General Strucural Representation of Newly Synthesized Nickel(II)-bis(quinoxaline-6,7-dithiolate) System

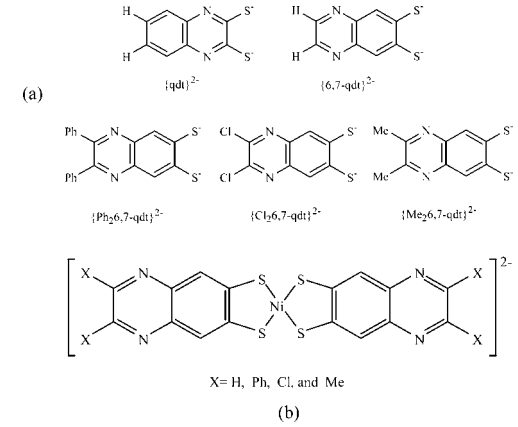

dithiolate-ligand [{6,7-qdt}$^{2-}$ = quinoxaline-6,7-dithiolate, Scheme 1a], and its nickel-square planar bis(dithiolene) complex $[Bu_4N]_2[Ni(6,7\text{-qdt})_2]$ (**1a**),[14] which has been useful to demonstrate the comparison of its electronic and electrochemical properties with those of existing well-established system $[Bu_4N]_2[Ni(qdt)_2]$. As a continuation, in the present contribution we wish to describe the effect of different substituents of the {6,7-qdt}$^{2-}$ ligand on the electronic properties of the $\{NiS_4\}$ group of $[Ni(6,7\text{-qdt})_2]^{2-}$. We are prompted to undertake this work by the landmark/classic publication of Gray and co-workers.[15a] They investigated systematically the effect of different substituents of dithiolato ligands on the electronic structure of $\{MS_4\}$ group in a series of metal complexes containing benzene 1,2-dithiolate and related ligands.[15a] A recent review article has described the 50-year old debate regarding the true electronic structure of transition metal bis(dithiolene) complexes that has been revolutionized by involvement of sulfur K-edge X-ray absorption spectroscopy to directly probe the sulfur composition of the frontier orbitals.[15b] We have reported three new quinoxaline based dithiolate-ligands ({$Ph_2$6,7-qdt}$^{2-}$, {$Cl_2$6,7-qdt}$^{2-}$, and{$Me_2$6,7-qdt}$^{2-}$) along with the reported dithiolate-ligand {6,7-qdt}$^{2-}$ (Scheme 1a) and their nickel square-planar bis(dithiolene) complexes. This new series of square-planar bis(dithiolene) complexes {$[Ni(X_2$6,7-qdt$)_2]$, Scheme 1b} give us an opportunity to carry out their comparative studies of electronic and electrochemical properties: $[Bu_4N]_2[Ni(6,7\text{-qdt})_2]$ (**1a**), $[PPh_4]_2[Ni(6,7\text{-qdt})_2]$ (**1b**), $[Bu_4N]_2[Ni(Ph_2$6,7-qdt$)_2]$ (**2a**), $[PPh_4]_2[Ni(Ph_2$6,7-qdt$)_2]\cdot$3DMF (**2b**), $[Bu_4N]_2[Ni(Cl_2$6,7-qdt$)_2]$ (**3**), $[Bu_4N]_2[Ni(Me_2$6,7-qdt$)_2]$ (**4**).

EXPERIMENTAL SECTION

Materials and Methods. All the chemicals for the synthesis were commercially available and used as received. 1,2-diaminobenzene-bis(thiocyanate) (**A**),[16] 2,3-diphenyl-6,7-bis-thiocyanato-quinoxaline (B),[17] 5,6-diamino-benzo[1,3]dithiole-2-thione (**C**),[18] quinoxaline-6,7-dithiol ($H_2$6,7-qdt) (**L_1**),[14] 2,3-diphenyl-quinoxaline-6,7-dithiol (L_2),[17] 6,7-dichloro-1,3-dithia-5,8-diaza-cyclopenta[b]naphthalen-2-one (**L_3**),[19] and $[Bu_4N]_2[Ni(6,7\text{-qdt})_2]$ (**1a**)[14] were prepared according to literature procedures. Syntheses of metal complexes were performed under N_2 using standard inert-atmosphere techniques. Solvents were dried by standard procedures.

Micro analytical (C, H, N) data were obtained with a FLASH EA 1112 Series CHNS Analyzer. Infrared (IR) spectra were recorded on KBr pellets with a JASCO FT/IR-5300 spectrometer in the region of 400−4000 cm^{-1}. ^{1}H NMR spectra of compounds were recorded on a Bruker DRX-400 spectrometer using $Si(CH_3)_4$ [TMS] as an internal standard. Electronic absorption spectra of solutions and diffuse reflectance spectra of solid compounds were recorded on a UV-3600 Shimadzu UV−vis−NIR spectrophotometer. A Cypress model CS-1090/CS-1087 electro analytical system was used for cyclic voltammetric experiments. The electrochemical experiments were measured in MeOH containing $[Bu_4N][ClO_4]$ as a supporting electrolyte using a Ag/AgCl electrode as a reference. We have used BAS MF-2013 model disk working platinum electrode with diameter 1.6 mm for measuring the electrode potentials. The potentials reported here are uncorrected for junction contributions.

Synthesis of 6,7-Dimethyl-1,3-dithia-5,8-diaza-cyclopenta-[*b*]naphthalen-2-thione (D). 5,6-Diamino-benzo[1,3]dithiole-2-thione (**C**) (150 mg, 0.7 mmol) and butane-2,3-dione (0.67 mL, 0.77 mmol) were dissolved in acetic acid (15.0 mL), and the reaction mixture was refluxed for 1.5 h. The resulting yellow precipitate was washed with MeOH several times and dried in vacuum to give a yellow colored solid. This compound can be directly used for the preparation of ligand L_4. Yield: 0.180 g (96.0%); Yellow solid; IR (KBr, cm^{-1}): 3059, 1450, 1398, 1321, 1182, 1068 (C═S), 883, 844, 758, 509, 424; ^{1}H NMR (400 MHz, $CDCl_3$): δ 8.08 (s, 2H), 2.77 (s, 6H) ppm; LC−MS (positive mode): m/z = 265 $[M^+{+}H]^+$; Anal. Calc. for $C_{11}H_8N_2S_3$: C, 49.97; H, 3.05; N, 10.60. Found: C, 50.23; H, 2.84; N, 10.85%.

Synthesis of 6,7-Dimethyl-1,3-dithia-5,8-diaza-cyclopenta-[*b*]naphthalen-2-one (L_4). To a solution of 6,7-dimethyl-1,3-dithia-5,8-diaza-cyclopenta[b]naphthalen-2-thione (**D**) (135 mg, 0.511 mmol) in chloroform and acetic acid (3:1, v/v, 40 mL), $Hg(OAC)_2$ (521 mg, 1.63 mmol) was added, and it was stirred for 12 h at room temperature under N_2 atmosphere. The precipitate was filtered off using Celite and washed with chloroform. The filtrate was extracted with saturated $NaHCO_3$ solution (3 × 33 mL) and water (50 mL). To remove any traces of water, anhydrous Na_2SO_4 was added. The solvent was removed in vacuum, which produces pale yellow colored compound L_4 as product. Yield: 115 mg (91.0%); pale yellow solid; IR (KBr, cm^{-1}): 3057, 2916, 1745 (C═O), 1653, 1454, 1398, 1319, 1178, 1093, 869, 844, 756, 582, 439; ^{1}H NMR (400 MHz, $CDCl_3$): δ 8.10 (s, 2H), 2.75 (s, 6H) ppm; LC−MS (positive mode): m/z = 249 $[M^+{+}H]^+$; Anal. Calc. for $C_{11}H_8N_2OS_2$: C, 53.20; H, 3.25; N, 11.28. Found: C, 53.67; H, 3.01; N, 10.98%.

Synthesis of $[PPh_4]_2[Ni(6,7\text{-qdt})_2]$ (1b). The dianion of 6,7-qdt was generated, in situ, by the reaction of quinoxaline-6,7-dithiol (**L_1**) (0.104 g, 0.536 mmol) with NaOH (0.060 g, 1.5 mmol) in MeOH (10 mL) under nitrogen atmosphere. To the resulting clear red solution, solid $NiCl_2\cdot6H_2O$ (0.064 g, 0.269 mmol) was added; the resulting dark red solution was stirred for 15 min at room temperature. Dark brown micro crystals were precipitated by adding tetraphenylphosphonium bromide (0.292 g, 0.696 mmol); the micro crystals were filtered, washed with water followed by a wash with diethyl ether, and dried at room temperature. It was recrystallized from acetonitrile solution by vapor diffusion with diethyl ether. Yield: 0.350 g (71.3% based on Ni). Anal. Calc. for $C_{64}H_{48}N_4S_4P_2Ni$: C, 68.51; H, 4.31; N, 4.99. Found: C, 68.23; H, 4.12; N, 5.36%. IR (KBR pellet) (υ/cm^{-1}): 3040, 1660, 1583, 1483, 1435, 1412, 1340, 1174, 1107, 1078, 1024, 925, 779, 752, 721, 688, 524; ^{1}H NMR (400 MHz, δ ppm) (CD_3CN): 7.67−7.76 (m, 40H), 7.90−7.93 (m, 8H).

Synthesis of $[Bu_4N]_2[Ni(Ph_2$6,7-qdt$)_2]$ (2a). The dianion of 2,3-diphenyl-6,7-qdt was generated, in situ, by the treatment of 2,3-diphenyl-quinoxaline-6,7-dithiol (**L_2**) (0.052 g, 0.15 mmol) with NaOH (0.020 g, 0.5 mmol) in methanol (7.0 mL). To the resulting clear red solution, solid $NiCl_2\cdot6H_2O$ (0.018 g, 0.075 mmol) was added; the resulting dark brown solution was stirred for 15 min at room temperature. Black colored micro crystals were precipitated by adding tetrabutylammonium bromide (0.07 g, 0.215 mmol); the micro crystals were filtered, washed with water followed by washing with diethyl ether, and dried at room temperature. It was recrystallized from acetonitrile solution by vapor diffusion with diethyl ether. Yield: 0.200 g (74.1% based on Ni). Anal. Calc. for $C_{72}H_{96}N_6S_4Ni$: C, 70.16; H, 7.85; N, 6.82. Found: C, 70.57; H, 7.29; N, 6.49%. IR (KBR pellet)

dx.doi.org/10.1021/ic301017g | Inorg. Chem. 2013, 52, 66−76

Table 1. Crystal Data and Structural Refinement for Complexes 1b, 2b, 3, and 4

	1b	2b	3	4
empirical formula	$C_{64}H_{48}N_4P_2S_4Ni$	$C_{97}H_{85}N_7O_3P_2S_4Ni$	$C_{48}H_{76}N_6S_4Cl_4Ni$	$C_{52}H_{88}N_6S_4Ni$
formula weight	1121.95	1645.61	1065.94	984.23
temperature (K)	100(2)	100(2)	100(2)	100(2)
crystal size (mm)	0.46 × 0.20 × 0.08	0.50 × 0.26 × 0.04	0.24 × 0.10 × 0.06	0.22 × 0.14 × 0.08
crystal system	monoclinic	monoclinic	monoclinic	triclinic
space group	$C2/c$	$C2/c$	$P2_1/c$	$P\bar{1}$
Z	4	8	2	2
wavelength (Å)	0.71073	0.71073	0.71073	0.71073
a [Å]	26.993 (2)	19.6540(12)	13.8484(15)	13.0326(11)
b [Å]	13.2302(9)	19.3493 (12)	8.5484(9)	14.3918(12)
c [Å]	16.4171(11)	41.897(3)	22.521(3)	15.8859(13)
α [deg]	90.000	90.000	90.000	114.6950(10)
β [deg]	117.476(2)	102.767(10)	101.239(3)	94.4320(10)
γ [deg]	90.000	90.000	90.000	100.2510(10)
volume [Å^3]	5201.6(7)	15539.2(17)	2614.9(5)	2625.3(4)
calculated density (Mg/m^{-3})	1.433	1.407	1.262	1.245
reflections collected/unique	27521/5393	79828/15262	23914/4580	27356/10289
R(int)	0.0548	0.0862	0.0771	0.0554
F(000)	2328	6896	988	1068
max. and min transmission	0.9504 and0.7563	0.9819 and0.8029	0.9552 and0.8366	0.9559 and 0.8850
Θ range for data collection (deg)	1.70 to 26.48	1.50 to 26.03	1.50 to 24.94	1.43 to 26.08
refinement method	full-matrix least-squares on F^2	full-matrix least-squares on F^2	full-matrix least-squares on F^2	full-matrix least-squares on F^2
data/restraints/parameters	5393/0/340	15262/0/972	4580/0/286	10289/0/580
goodness-of-fit on F^2	1.112	1.112	1.249	1.089
R_1/wR_2 [$I > 2\sigma(I)$]	0.0804/0.1970	0.0875/0.1805	0.1690/0.3640	0.0786/0.1801
R_1/wR_2 (all data)	0.0921/0.2052	0.1120/0.1924	0.1830/0.3733	0.1049/0.1942
largest diff. peak and hole [e Å^{-3}]	1.834 and −0.449	0.821 and −0.984	1.377 and −0.791	1.910 and −0.451

(υ/cm^{-1}): 2959, 2918, 2860, 1595, 1483, 1423, 1340, 1192, 1072, 1024, 858, 821, 698. ^{1}H NMR (400 MHz, δ ppm) (CD_3CN): 0.949 (t, 24H), 1.32−1.37 (m, 16H), 1.60 (bs, 16H), 3.10 (t, 16H), 7.15−7.37 (m, 24H).

Synthesis of $[PPh_4]_2[Ni(Ph_2$6,7-qdt$)_2]\cdot$3DMF (2b). This compound was prepared by using above procedure, used for the preparation of compound **2a**, but tetraphenylphosphonium bromide was added in place of tetrabutylammonium bromide. The solid thus obtained was recrystallized from DMF solution by vapor diffusion with diethyl ether. Yield: 79.4% based on Ni. Anal. Calc. for $C_{97}H_{85}N_7O_3P_2S_4Ni$: C, 70.79; H, 5.21; N, 5.96. Found: C, 70.25; H, 5.34; N, 6.18%. IR (KBR pellet) (υ/cm^{-1}): 3059, 2953, 2924, 1670, 1425, 1340, 1195, 1107, 1082, 1020, 723, 690, 520; ^{1}H NMR (400 MHz, δ ppm) (CD_3CN): 7.31−7.48 (m, 20H), 7.70−7.77 (m, 40H), 7.90−7.93 (m, 4H).

Synthesis of $[Bu_4N]_2[Ni(Cl_2$6,7-qdt$)_2]$ (3). The dianion of 2,3-dichloro-6,7-qdt was generated, in situ, by the treatment of 6,7-dichloro-1,3-dithia-5,8-diaza-cyclopenta[b]naphthalen-2-one (L_3) (0.080 g, 0.277 mmol) with Na metal (0.020 g, 0.877 mmol) in methanol (10 mL). To the resulting clear brown solution, solid $NiCl_2\cdot 6H_2O$ (0.034 g, 0.143 mmol) was added, and it was stirred for 15 min at room temperature. To this, tetrabutylammonium bromide (0.1 g, 0.310 mmol) was added followed by the addition 30 mL of deionized water that results in the precipitation of black colored micro crystals; the micro crystals were filtered, washed with water followed by washing with diethyl ether, and dried at room temperature. It was recrystallized from acetonitrile solution by vapor diffusion with diethyl ether. Yield: 0.190 g (52.9% based on Ni). Anal. Calc. for $C_{48}H_{76}N_6S_4Cl_4Ni$: C, 54.09; H, 7.19; N, 7.88. Found: C, 54.41; H, 7.25; N, 7.51%. IR (KBR pellet) (υ/cm^{-1}): 2959, 2872, 1562, 1433, 1377, 1315, 1194, 1149, 1078, 983, 862, 738, 570, 518. ^{1}H NMR (400 MHz, δ ppm) (CD_3CN): 0.946 (t, 24H), 1.34 (bs, 16H), 1.59 (bs, 16H), 3.08 (t, 16H), 7.42 (s, 4H).

Synthesis of $[Bu_4N]_2[Ni(Me_2$6,7-qdt$)_2]$ (4). The dianion of 2,3-dimethyl-6,7-qdt was generated, in situ, by the reaction of 6,7-dimethyl-1,3-dithia-5,8-diaza-cyclopenta[b]naphthalen-2-one (L_4) (0.100 g, 0.401 mmol) with Na (0.046 g, 2.0 mmol) in MeOH (10 mL) under nitrogen atmosphere. To the resulting clear red solution, $NiCl_2\cdot 6H_2O$ (0.048 g, 0.201 mmol) was added, and the dark red solution obtained was stirred for 15 min at room temperature. Dark red micro crystals were precipitated by adding tetrabutylammonium bromide (0.2 g, 0.621 mmol); the micro crystals were filtered, washed with water followed by washing with diethyl ether, and finally microcrystals were dried at room temperature. It was recrystallized from acetonitrile solution by vapor diffusion with diethyl ether. Yield: 0.295 g (71.2% based on Ni). Anal. Calc. for $C_{52}H_{88}N_6S_4Ni$: C, 63.46; H, 9.01; N, 8.54. Found: C, 63.25; H, 8.89; N, 8.81%. IR (KBR pellet) (υ/cm^{-1}): 2957, 2924, 2866, 1736, 1635, 1570, 1448, 1423, 1325, 1168, 1076, 989, 839, 748, 588; ^{1}H NMR (400 MHz, δ ppm) (CD_3CN): 0.93 (bs, 24H), 1.32 (bs, 16H), 1.58 (bs, 16H), 2.56 (s, 12H) 3.09 (bs, 16H), 8.15 (s, 4H).

X-ray Crystallography. Single crystals, suitable for facile structural determination for all the compounds **1b**, **2b**, **3**, and **4**, were measured on a three circle Bruker SMART APEX CCD area detector system under Mo−Kα (λ = 0.71073 Å) graphite monochromatic X-ray beam. The frames were recorded with an ω scan width of 0.3°, each for 10 s, crystal-detector distance 60 mm, collimator 0.5 mm. Data reduction was performed by using SAINTPLUS.[20] Empirical absorption corrections were done using equivalent reflections performed program SADABS.[20] The structures were solved by direct methods and least-squares refinement on F^2 for all the compounds by using SHELXS-97.[21] All non-hydrogen atoms were refined anisotropically. The hydrogen atoms were included in the structure factor calculation by using a riding model. The crystallographic parameters, data collection, and structure refinement of the compounds **1b**, **2b**, **3**, and **4** are summarized in Table 1. Selected bond lengths and angles for the compounds **1b**, **2b**, **3**, and **4** are listed in Table 2.

Computational Details. Electronic structure calculations of the ground state of the **1a**, **2b**, **3**, and **4** complex anions have been performed using density functional theory (DFT) methods employing the G03 suite of program.[22] The functional used throughout this study is the B3LYP,[23] consisting of the nonlocal hybrid exchange functional

dx.doi.org/10.1021/ic301017g | Inorg. Chem. 2013, 52, 66−76

Table 2. Selected Bond Lengths and Bond Angles of the Compounds Presented in the Study[a]

		Compound **1b**	
Ni(1)−S(2)#1	2.1578(11)	Ni(1)−S(2)	2.1578(11)
Ni(1)−S(1)#1	2.1664(12)	Ni(1)−S(1)	2.1665(12)
S(2)#1−Ni(1)−S(2)	180.00(6)	S(2)#1−Ni(1)−S(1)#1	91.35(4)
S(2)−Ni(1)−S(1)#1	88.65(4)	S(2)#1−Ni(1)−S(1)	88.65(4)
S(2)−Ni(1)−S(1)	91.35(4)	S(1)#1−Ni(1)−S(1)	180.00(4)
C(1)−S(1)−Ni(1)	104.89(15)	C(2)−S(2)−Ni(1)	104.92(15)
		Compound **2b**	
Ni(1)−S(1)	2.1592(13)	Ni(1)−S(4)	2.1622(13)
Ni(1)−S(2)	2.1746(13)	Ni(1)−S(3)	2.1746(13)
S(1)−Ni(1)−S(4)	178.36(6)	S(1)−Ni(1)−S(2)	91.54(5)
S(4)−Ni(1)−S(2)	88.53(5)	S(1)−Ni(1)−S(3)	88.51(5)
S(4)−Ni(1)−S(3)	91.48(5)	S(2)−Ni(1)−S(3)	177.81(6)
C(1)−S(1)−Ni(1)	105.29(16)	C(21)−S(3)−Ni(1)	105.61(15)
C(22)−S(4)−Ni(1)	105.56(16)	C(2)−S(2)−Ni(1)	105.24(16)
		Compound **3**	
Ni(1)−S(2)	2.160(3)	Ni(1)−S(2)#2	2.160(3)
Ni(1)−S(1)#2	2.163(3)	Ni(1)−S(1)	2.163(3)
S(2)−Ni(1)−S(2)#2	179.998(1)	S(2)−Ni(1)−S(1)#2	88.42(10)
S(2)#2−Ni(1)−S(1)#2	91.58(10)	S(2)−Ni(1)−S(1)	91.58(10)
S(2)#2−Ni(1)−S(1)	88.42(10)	S(1)#2−Ni(1)−S(1)	180.0
C(1)−S(1)−Ni(1)	105.8(4)	C(2)−S(2)−Ni(1)	105.4(4)
		Compound **4**	
Ni(1)−S(4)	2.1599(12)	Ni(1)−S(2)	2.1675(12)
Ni(1)−S(1)	2.1699(12)	Ni(1)−S(3)	2.1786(12)
S(4)−Ni(1)−S(2)	177.89(5)	S(4)−Ni(1)−S(1)	87.93(4)
S(2)−Ni(1)−S(1)	90.83(4)	S(4)−Ni(1)−S(3)	91.22(4)
S(2)−Ni(1)−S(3)	90.15(4)	S(1)−Ni(1)−S(3)	175.30(5)
C(1)−S(1)−Ni(1)	105.77(14)	C(6)−S(2)−Ni(1)	105.55(14)
C(16)−S(4)−Ni(1)	105.91(15)	C(11)−S(3)−Ni(1)	105.20(15)

[a]Symmetry transformations used to generate equivalent atoms: #1 $-x+1/2,-y+3/2,-z+1$; #2 $-x+2,-y+2,-z$.

as defined by Becke 3-Parameter (exchange) and nonlocal Lee, Yang, and Parr correlation functional. The LanL2DZ basis set is used for the Ni atom including LanL2 effective core-potential (ECP), and for the remaining atoms the 6-311G** basis set is used. The ground-state anionic complexes are obtained in the methanol phase by full geometry optimization and also frequency calculations. The optimized structures located as saddle points on the potential energy surfaces were verified by the absence of imaginary frequencies. Vertical excited state calculations are performed with the TD-B3LYP method using the same basis functions mentioned in the above. The details of computational output are described in the Supporting Information.

RESULTS AND DISCUSSION

Synthesis and General Characterization. The synthetic routes for the synthesis of four dithiolate-ligands $\mathbf{L_1}$−$\mathbf{L_4}$ have been shown in Scheme 2. The synthetic procedure of dithiolate-ligands $\mathbf{L_1}$ and $\mathbf{L_2}$ has been reported in our earlier publications as shown in Scheme 2a.[14,17] In our previous letter,[19] the synthesis of dithiolate-ligand $\mathbf{L_3}$ has been described; the relevant synthesis starts from 5,6-diamino-benzo[1,3]-dithiole-2-thione as shown in Scheme 2b. Likewise, dithiolate-ligand $\mathbf{L_4}$ has been obtained in two steps, starting from 5,6-diamino-benzo[1,3]dithiole-2-thione (**C**). In the first step, 6,7-dimethyl-1,3-dithia-5,8-diaza-cyclopenta[*b*]naphthalen-2-thione (**D**) was prepared according to a modifed literature procedure[24] that is described by the condensation reaction of 5,6-diamino-benzo[1,3]dithiole-2-thione (**C**) with butane-2,3-dione in acetic acid at refluxing conditions (Scheme 2b). In the second step of the synthesis, the 1,3-dithia-2-thione derivative (**D**) is converted into corresponding 1,3-dithia-2-one derivative ($\mathbf{L_4}$) by using $Hg(OAc)_2$ in $CHCl_3$:CH_3COOH (3:1) as shown in Scheme 2b. All these synthesized organic compounds have been characterized by NMR spectroscopy including elemental and LC-MS analyses (see Supporting Information for relevant plots).

Syntheses of metal complexes have been performed using a general procedure as shown in Scheme 3. The $\{X_2$6,7qdt$\}^{2-}$ ions are generated, in situ, by the reaction of ligands ($\mathbf{L_1}$−$\mathbf{L_4}$) in basic medium containing MeOH solution, which are subsequently reacted with nickel chloride salt resulting in the formation of the respective nickel complexes and precipitated/isolated as tetrabutylammonium salts by the addition of $[Bu_4N]$Br [compounds **1a**, **2a**, **3**, and **4**]. Tetraphenylphosphonium bromide is added instead of adding tetrabutylammonium bromide for the precipitation of nickel complexes of ligands $\mathbf{L_1}$ and $\mathbf{L_2}$ resulting in the isolation of compounds **1b** and **2b**, respectively as shown in Scheme 3a. Metal complexes **1a**, **1b**, **2a**, **3**, and **4** are recrystallized from acetonitrile solution by the vapor diffusion of diethyl ether. Compound **2b** is recrystallized from DMF solution by the vapor diffusion of diethyl ether. Crystals of compounds **1a**, **1b**, **2b**, **3**, and **4** have been characterized by single crystal X-ray structure determination. The crystals of compound **2a** are not suitable for single crystal X-ray structure analysis. All the metal coordination complexes have been further characterized by NMR spectroscopy including their elemental analysis.

Electronic Absorption Spectra. The electronic absorption spectra of complexes **1a**, **2a**, **3**, and **4** in MeOH solutions are shown in Figure 1a. The broad bands are observed in the visible region centered at ∼588 nm (ε = 35000 L mol^{-1} cm^{-1}), ∼607 nm (ε = 21,000 L mol^{-1} cm^{-1}), ∼610 nm (ε = 34,600 L mol^{-1} cm^{-1}), and ∼547 nm (ε = 24,200 L mol^{-1} cm^{-1}) for complexes **1a**, **2a**, **3**, and **4**, respectively. The corresponding solid state diffuse reflectance spectra are shown in Figure 1b. Molecular orbital calculations, reported for metal bis-(dithiolato) complexes, indicate the lowest energy charge transfer (CT) state involves a highest occupied molecular orbital (HOMO) which is a mixture of dithiolate (π) and metal (d) orbital character; the relative contribution depend on the metal ion, type of dithiolate chelate and charge of the concerned complex.[25] For the complex anion $[Pt(mnt)_2]^{2-}$, the CT transition was assigned to involve a HOMO (having a large dithiolate ligand contribution and small metal "d" orbital contribution) and a lowest unoccupied molecular orbital (LUMO) of π^* (dithiolate) participation.[11a,25g] However, in the case of $[Ni(mnt)_2]^{2-}$, the HOMO is characterized by dithiolate-centered orbitals without metal-d contribution, and the LUMO is a mixture of dithiolate (π) and metal (d)

dx.doi.org/10.1021/ic301017g | *Inorg. Chem.* 2013, 52, 66−76

Scheme 2. Synthesis of Quinoxaline Dithiolate Ligands (a) L_1 and L_2; (b) L_3 and L_4

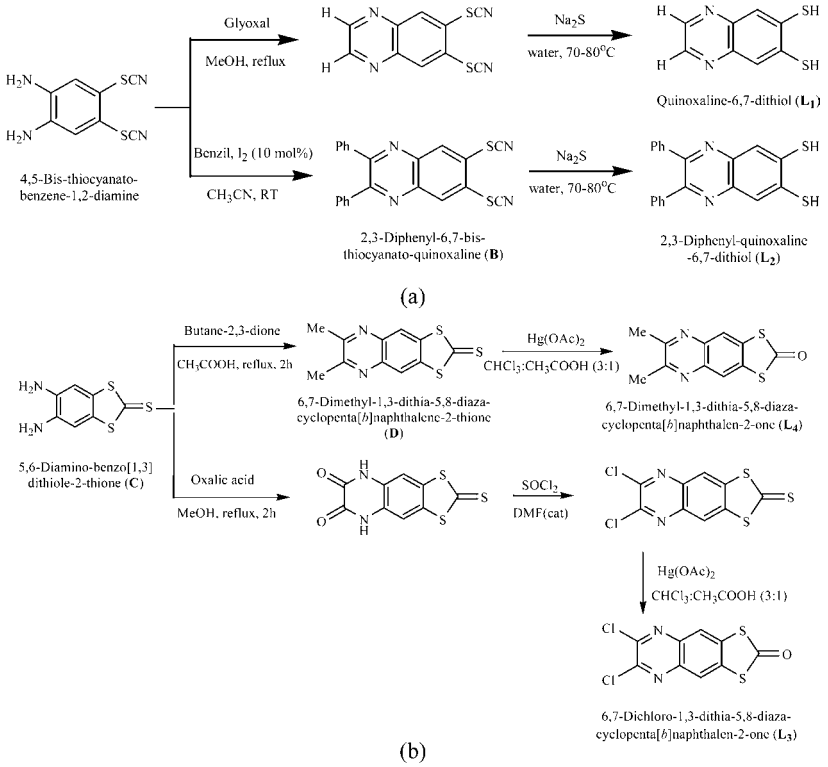

Scheme 3. Synthesis of Nickel 6,7-Quinoxaline-dithiolate Complexes (a) 1a, 1b, 2a, and 2b; (b) 3 and 4

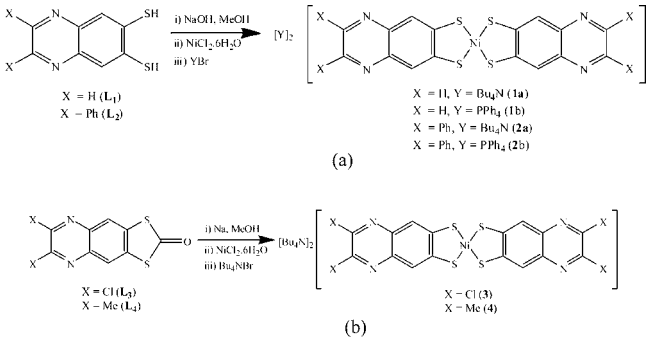

orbitals.[26] Cummings and Eisenberg reported electronic transition for $[Pt(qdt)_2]^{2-}$ (a complex anion with a ligand, related to the present study) and described the lowest-energy excited state as a mixture of MLCT and dithiolate intraligand (IL) character.[11a] We performed ground state electronic structure calculations for $[Ni(6,7\text{-qdt})_2]^{2-}$ (in **1a**), $[Ni(Ph_2 6,7\text{-qdt})_2]^{2-}$ (in **2b**), $[Ni(Cl_2 6,7\text{-qdt})_2]^{2-}$ (in **3**), and $[Ni(Me_2 6,7\text{-qdt})_2]^{2-}$ (in **4**) using density functional theory (DFT) methods (see computational details in Experimental Section). From the vertical excitation energy data for these complex anions, the first absorption originates from respective HOMO to LUMO, where HOMOs are of π type character and LUMOs are of π^* type character. The resulting HOMO and LUMO diagrams are shown in Figure 2. By careful investigation

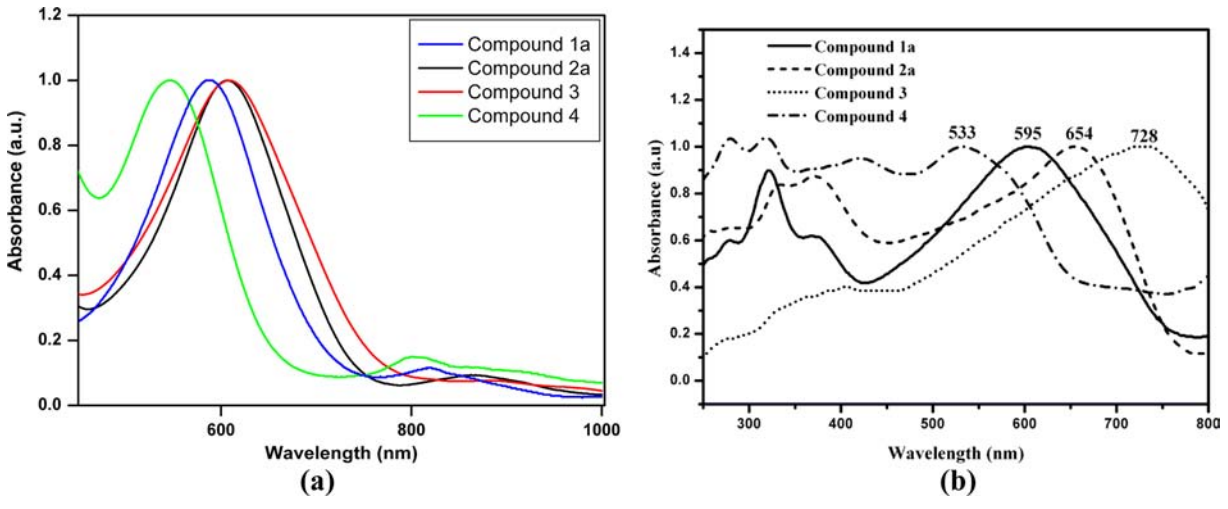

Figure 1. (a) Electronic absorption spectra in MeOH solutions and (b) diffuse reflectance spectra of solid compounds **1a**, **2a**, **3**, and **4**.

dx.doi.org/10.1021/ic301017g | Inorg. Chem. 2013, 52, 66−76

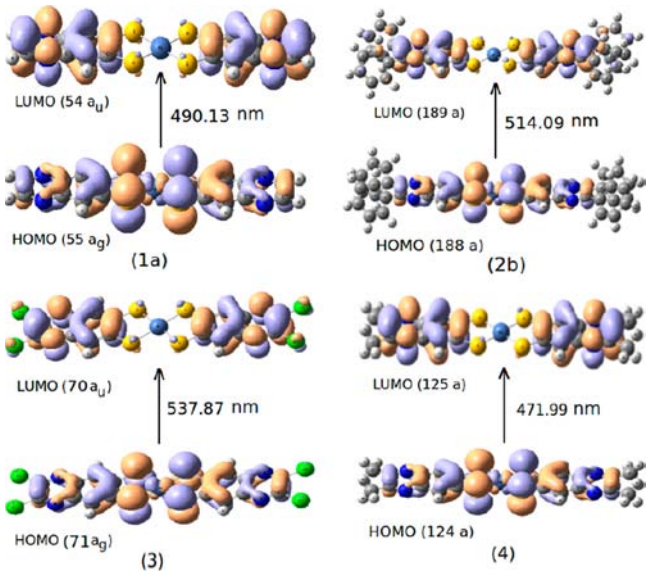

Figure 2. HOMO and LUMO diagrams originated from molecular orbital calculations for the anions of compounds **1a**, **2b**, **3**, and **4**.

on the MO picture (Figure 2), we found a small contribution of the central metal in the HOMOs and in the LUMOs, the electron density is high in the π^* orbitals of dithiolate. Since the HOMO includes metal-mixed ligand-based orbitals, we state that the transitions are "mixed-metal ligand-to-ligand" CT, as also mentioned for the (diimine)Pt(dithiolene) complexes.[11a] The calculated vertical transition wavelengths for the complex anions $[Ni(6,7\text{-qdt})_2]^{2-}$ (in **1a**), $[Ni(Ph_2 6,7\text{-qdt})_2]^{2-}$ (in **2b**), $[Ni(Cl_2 6,7\text{-qdt})_2]^{2-}$ (in **3**), and $[Ni(Me_2 6,7\text{-qdt})_2]^{2-}$ (in **4**) are 490.13 nm, 514.09 nm, 537.87, and 471.99 nm, respectively. These findings follow the same trend as we observed in the experiment (the electronic absorption spectra of complexes **1a**, **2a**, **3**, and **4** in MeOH solutions as shown in Figure 1a). Thus the origin of the electronic transition (broad band in the visible region) of the present system ($[Ni(X_2 6,7\text{-qdt})_2]^{2-}$; X = H, Ph, Cl, and Me) is analogous to that of $[Pt(qdt)_2]^{2-}$, as reported by Cummings and Eisenberg.[11a]

It is evident from the electronic absorption spectral studies (Figure 1, Table 3) in solution as well as in solid state that

Table 3. Influences of the Nature of the Electron Donating and Withdrawing Groups on the Shifting of Absorption Position Maxima of the CT Bands in the Visible Region

		CT band of the compounds, λ_{max} (nm)			
S.No	solvent/solid	**1a**	**2a**	**3**	**4**
1	MeOH	588	607	609	547
2	DCM	593	623	642	560
3	acetonitrile	593	624	640	566
4	DMF	619	662	707	593
5	acetone	619	660	709	589
6	solid-state	595	654	728	533

electron donating groups (e.g., methyl group of compound **4**) alter the position of the absorption maxima toward the blue region and electron-withdrawing groups (e.g., chloro and phenyl groups in compounds **3** and **2a**, respectively) shift the position of the absorption maxima to the red region. This trend is consistent in the solid state even more profoundly as shown Figure 1b (diffuse reflectance spectra). The influence of a particular substituent on an aromatic system can usually be understood in terms of inductive as well as mesomeric effects.[27] The mesomeric effect comes from the delocalization of the π-electrons between aromatic core and the substituent. Thus in the present study, the mesomeric effect is important in the case of compounds $[Bu_4N]_2[Ni(Ph_2 6,7\text{-qdt})_2]$ (**2a**) and $[PPh_4]_2[Ni(Ph_2 6,7\text{-qdt})_2]\cdot 3DMF$ (**2b**), where substituted phenyl group can share π-electrons (by resonance) with aromatic core having dithiolato ligands. The inductive effect is fully associated with the σ-electron system of the aromatic molecule. The electron withdrawing group (for example, Cl atom as a substituent) pulls electron density by the inductive effect and lowers the energies of the highest occupied and lowest unoccupied π-MOs. This is because the electron acceptors withdraw some electron density from the ligands, thereby reducing the repulsive Coulombic interaction between the electrons occupying the ligand-localized π-MOs and the electrons of the σ-system. In the present system, we have established (by molecular orbital calculations and comparing with other similar systems) that the HOMO is a mixture of dithiolate (π) and metal (d) orbital character and the LUMO is a π^* orbital of the dithiolate ligand. Thus an electron withdrawing substituent on the heterocyclic dithiolate ligand (present system) causes lowering the energy of LUMOs because these are purely π-MOs of dithiolate ligand without lowering the energy of HOMOs considerably (these are mixture of nickel d-orbital character and dithiolate π-type). This results in decreasing the energy gap between HOMO and LUMO. This explains why electron withdrawing groups (substituents $-Cl$ and $-C_6H_5$ in compounds **3** and **2a** respectively) cause red shift in their electronic absorption spectra (Table 3). The red shift of the absorption maximum of the phenyl-substituted compound **2a** indicates that the inductive effect is dominant over mesomeric effect. On the other hand, electron donating group (for example substituent $-CH_3$ in compound **4**) increases the electron density toward dithiolate ligand and thereby increases the repulsive Coulombic interaction between ligand centered π-MOs and σ-electrons. As a result, the energy of LUMOs will rise and the energy gap between HOMO and LUMO will increase. This is why the methyl substituted dithiolate complex exhibits blue shift in its electronic absorption spectrum (Table 3). As shown in Figure 1a, there are some small features beyond 800 nm (820 nm for compound **1a**, 865 nm for compound **2a**, 890 nm for compound **3** and 800 nm for compound **4**). These small features might be due to the radical anion species formed by aerial oxidation of the corresponding $[Ni(X_2\text{-}6,7\text{-qdt})_2]$ dianions, which is not surprising because of low oxidation potential of the present system.

Furthermore, the CT bands of all these complexes are sensitive to the solvent polarity of the solvents as shown in Table 3. In DMF and acetone solvents, the CT bands are observed in the lower energy region; on other hand in DCM and acetonitrile solvents, the CT bands absorb at the higher energy region for all the complexes **1a**, **2a**, **3**, and **4**.

Electrochemistry. Interestingly, complexes **1a**, **2a**, **3**, and **4** undergo reversible oxidation at very low oxidation potentials in MeOH solutions as shown in Figure 3. We have shown in our earlier communication[14] that complex **1a** undergoes $E_{1/2}$ = +0.12 V vs Ag/AgCl (ΔE = 74 mV) corresponding to $[Ni(6,7\text{-qdt})_2]^{-}/[Ni(6,7\text{-qdt})_2]^{2-}$ redox couple, which is less as compared to the first oxidation potential for the complex $(Bu_4N)_2[Ni(qdt)_2]$ appearing at $E_{1/2}$ = +0.41 V vs Ag/AgCl

dx.doi.org/10.1021/ic301017g | Inorg. Chem. 2013, 52, 66−76

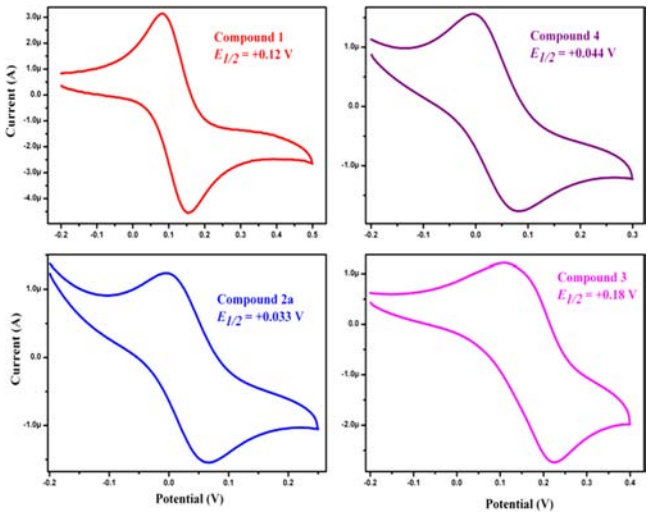

Figure 3. Cyclic voltammograms of compounds **1a**, **2a**, **3**, and **4** in MeOH solutions at scan rate 50 mV s^{-1}, V vs Ag/AgCl.

(ΔE = 89 mV), that corresponds the $[Ni(qdt)_2]^-/[Ni(qdt)_2]^{2-}$ redox couple in the electrochemical scale. We have also mentioned that complex **1a** is easily oxidized from dianion to monoanion compared to the $(Bu_4N)_2[Ni(qdt)_2]$ complex. To answer the question of why $[Ni(H_2\text{-}6,7\text{-}qdt)_2]^{2-}$ has much lower oxidation potential than that of $[Ni(qdt)_2]^{2-}$, we argue that the electron accepting ability of the ring N atoms in $[Ni(qdt)_2]^{2-}$ should be more than that of the ring N atoms in $[Ni(H_2\text{-}6,7\text{-}qdt)_2]^{2-}$ because the ring N atoms are closer to $\{NiS_4\}$ core in $[Ni(qdt)_2]^{2-}$ than those in $[Ni(H_2\text{-}6,7\text{-}qdt)_2]^{2-}$. If the electron density of the $\{NiS_4\}$ core is pulled more toward the ligand (as in the case of $[Ni(qdt)_2]^{2-}$), the concerned $\{NiS_4\}$ moiety should not be oxidized easily. On the other hand, in the case of $[Ni(H_2\text{-}6,7\text{-}qdt)_2]^{2-}$, because of the longer distance of the ring N acceptors from the nickel ion, the electron density in $\{NiS_4\}$ core is not pulled toward the ligand that effectively. Consequently, the $[Ni(H_2\text{-}6,7\text{-}qdt)_2]^{2-}$can be relatively easily oxidized. Thus the difference of ring N position between 6,7-qdt and normal qdt explains the shift of oxidation potential.

The first oxidation potentials for the complexes **2a**, **3**, and **4** appear at $E_{1/2}$ = +0.033 V (ΔE = 65 mV), $E_{1/2}$ = +0.18 V (ΔE = 77 mV) and $E_{1/2}$ = +0.044 V (ΔE = 89 mV) vs Ag/AgCl, respectively, as shown in Figure 2. These oxidations correspond to the dianionic complex to monoanionic complex of **2a**, **3**, and **4**, respectively. In addition, compounds **1a**, **2a**, **3**, and **4** show some irreversible oxidations as shown in Table 4, and the relevant CV diagrams are shown in the Supporting Information, Figures S1, S2, S3, S4.

The effect of substituents of the aromatic ring having dithiolate ligands attached to the $\{NiS_4\}$ core on the oxidation potential of the complex anion can be explained by inductive- and mesomeric-effects of the substituents. In the present study, only the phenyl-substituted system (compounds **2a** and **2b**) should have a mesomeric effect because the π-electrons of the phenyl group can undergo delocalization with π-electrons of the aromatic ring. On the other hand, the substituents of compounds **3** and **4** should have an inductive effect because in compound $[Bu_4N]_2[Ni(Cl_2 6,7\text{-}qdt)_2]$ (**3**) there is an electron withdrawing substituent (chlorine atom), which can pull electron density from the $\{NiS_4\}$ core and in compound $[Bu_4N]_2[Ni(Me_2 6,7\text{-}qdt)_2]$ (**4**), the substituted methyl group is electron donating, that will push/increase the electron density toward the $\{NiS_4\}$ core. Thus expectedly, the first oxidation potential of compound **3** is higher than that of compound **1a** (the relevant $\{NiS_4\}$ moiety is difficult to oxidize, because the metal electron will have a tendency to shift toward the electron withdrawing substituent). For the same reason, compound **4** will have relatively less potential (because the relevant $\{NiS_4\}$ core is easy to oxidize because the electron donating methyl group would increase the electron density toward the metal ion). In the case of compound **2a** (or **2b**), both inductive- and mesomeric- effects are possible; however in the electrochemical cell, the mesomeric effect dominates over the inductive effect and that is why it exhibits a relatively lower oxidation potential (relevant metal center is easy to oxidize because of electron pushing tendency toward metal ion through delocalization of π-electrons between phenyl group and aromatic ring). This is in contrast to the electronic absorption spectroscopy where the inductive effect in compound **2a** (or **2b**) prevails (vide supra).

Table 4. Electrochemical Data of the Compounds 1a, 2a, 3, and 4

	1a	2a	3	4
$E^1{}_{1/2}{}^{oxd}$ (V)	+0.12(rev)	+0.033(rev)	+0.18(rev)	+0.044(rev)
$E^{2\ oxd}$ (V)	+0.27(irr)		+0.32(irr)	
$E^{3\ oxd}$ (V)	+0.58(irr)	+0.36(irr)	+0.49(irr)	+0.57(irr)

Description of the Crystal Structures. The structural details of compound $[Bu_4N]_2[Ni(6,7\text{-}qdt)_2]$ (**1a**) have been reported in our earlier communication.[14]

*$[PPh_4]_2[Ni(6,7\text{-}qdt)_2]$ (**1b**).* The crystals of compound **1b**, suitable for single crystal X-ray structure determination, were obtained from acetonitrile solution by the vapor diffusion of diethyl ether. Crystallographic analysis revealed that compound **1b** crystallizes in the monoclinic system with space group $C2/c$ whereas compound **1a** crystallizes in $P2(1)/c$.[14] The asymmetric unit in the crystal structure of compound **1b** contains a half molecule of $[Ni(6,7\text{-}qdt)_2]^{2-}$ anion and one tetraphenylphosphonium cation. A thermal ellipsoid plot of compound **1b** containing the anion complex unit is shown in Figure 4a. Even though, both complex anions in **1a** and **1b** form almost square planar geometry around the Ni^{2+} ion, which is coordinated by four sulfur atoms from two 6,7-qdt^{2-} ligands between the two SMS planes, there is more deviation in the planarity of the

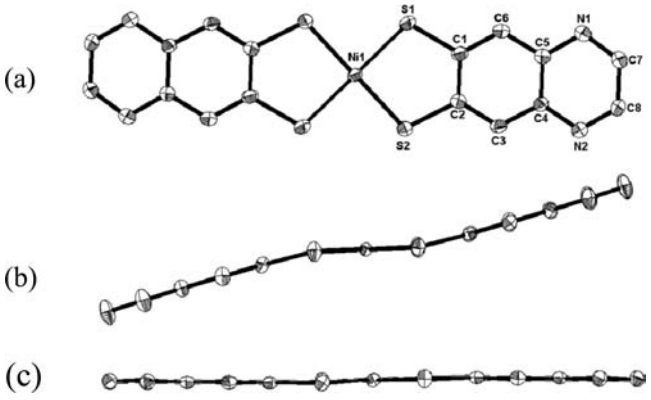

Figure 4. (a) Thermal ellipsoidal diagram of compound **1b** containing complex unit (40% probability); sideview representation of complexes (b) **1b** and (c) **1a**.

dx.doi.org/10.1021/ic301017g | *Inorg. Chem.* 2013, 52, 66−76

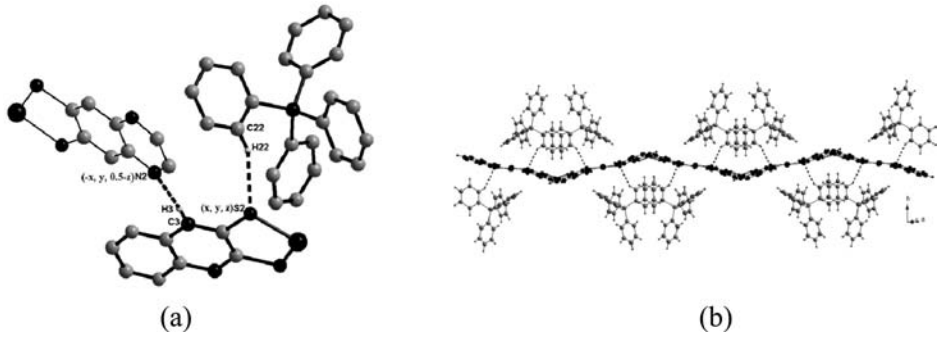

Figure 5. (a) View of the asymmetric unit of $[PPh_4]_2[Ni(6,7\text{-qdt})_2]$ (**1b**) (thick solid lines) (some of the hydrogen atoms are removed for clarity) showing all the H-bonding intermolecular cation−anion and anion−anion contacts (dotted lines) with other surrounding moieties (thin solid lines); (b) One dimensional supramolecular chain of compound **1b** characterized by C−H···N and C−H···S weak interactions.

dithiolate-chelate present in the complex **1b**; on the other hand, the crystal structure of compound **1a** shows less deviation as shown in Figures 4b and 4c. The coordination angles are in the range of 88.41(13)°−91.59(13)° in complex **1a** and 88.65(4)°−91.35(4)° in complex **1b**, which are very close to 90.0°, and other coordination angles are 180.0° in both the complexes **1a** and **1b**, which are not deviated. The bending deviation (η) between the SMS plane and SCCS plane are characterized by the angle of 11.93° present in the {Ni1S1S2C1C2} chelate of the complex **1b**, whereas in complex **1a** this bending deviation is 1.88°. This deviation in planarity of the dithiolate-chelate might be due to the involvement of S atoms in C−H···S weak interactions with cation−anion contacts, as shown in Figure 5a. In the crystal structure of compound **1b**, both cation $[Ph_4P]^+$ and anion $[Ni(6,7\text{-qdt})_2]^{2-}$ are involved in C−H···S and C−H···N hydrogen bonding interactions resulting in a one-dimensional supramolecular chainlike arrangement (Figure 5b).The relevant hydrogen bonding geometrical parameters are listed in the Table 5. This supramolecular chain engages C−H···S weak hydrogen bonding interactions with surrounding tetraphenylphosphonium cations as shown in Figure 5b.

*$[PPh_4]_2[Ni(Ph_2$6,7-qdt$)_2]\cdot$3DMF (**2b**).* The crystals of compound **2b**, suitable for single crystal X-ray structure determination, were obtained from DMF solution by the vapor diffusion of diethyl ether. Compound **2b** crystallizes in monoclinic space group $C2/c$. The asymmetric unit of compound **2b** contains one molecule of $[Ni(Ph_2$6,7-qdt$)_2]^{2-}$ and two tetraphenylphosphonium cations as shown in Supporting Information, Figure S5a. In addition to this, three DMF solvent molecules are crystallized in the crystal lattice of the compound **2b**, in which, two of them are present in 2-fold axis of symmetry. These two DMF solvent molecules suffer from significant disorder; thus we could not perform anisotropic refinement for these two solvent molecules as shown in the Supporting Information, Figure S5b. Thermal ellipsoidal diagram of the complex anion $[Ni(Ph_2$6,7-qdt$)_2]^{2-}$ in compound **2b** is shown in Figure 6a. The dihedral angle between the two SMS planes is 2.70° and the geometry around the Ni^{2+} ion, which is coordinated by four sulfur atoms from two {$Ph_2$6,7-qdt} ligands, shows slightly distorted from square planar geometry as shown in Figure 6b. The coordination angles are in the range of 177.81(6)°−178.36(6)° and 88.51(5)°−91.51(5)°, which are slightly deviated from angles of 180.0° and 90.0°, respectively. In addition to the dihedral angle, complex **2b** shows bending deviations (from planarity) of the dithiolate-chelates. The bending deviations (η) between the {S1Ni1S2} and {S1C1C2S2} planes, and {S3Ni1S4} and {S3C21C22S4} planes, are characterized by the angles of 5.80°and 0.26° present in {Ni1S1S2C1C2} and {Ni1S3S4C21C22} dithiolate-chelates, respectively. The crystal structure of the compound **2b** is characterized by three C−H···S weak interactions and one C−H···N weak interaction between the anion and the cations resulting in a one-dimensional supramolecular chain as shown Figure 6c. The weak C−H···S interactions may cause the deviation of dihedral angles around the metal ion and bending deviation of dithiolene-chelated ring.

Table 5. Hydrogen Bonds for the Complexes 1b, 2b, and 4[a]

D−H···A	d(D-H)	d(H···A)	d(D···A)	∠(DHA)
	Compound **1b**			
C(3)−H(3)···N(2)[b]	0.93	2.61	3.531(6)	170.1
C(22)−H(22)···S(2)	0.93	2.88	3.650(6)	141.4
	Compound **2b**			
C(76)−H(76)···S(2)[c]	0.93	2.99	3.769(6)	142.9
C(61)−H(61)···S(1)[c]	0.93	2.94	3.801(5)	154.8
C(60)−H(60)···S(3)[c]	0.93	2.91	3.722(5)	147.3
C(54)−H(54)···O(1)[d]	0.93	2.62	3.469(6)	152.9
C(48)−H(48)···O(1)[d]	0.93	2.68	3.583(6)	164.6
C(50)−H(50)···N(4)[e]	0.93	2.72	3.576(6)	153.8
C(12)−H(12)···O(1)[f]	0.93	2.68	3.316(6)	125.8
	Compound **4**			
C(25)−H(25A)···S(2)[g]	0.97	2.86	3.814(4)	167.1
C(21)−H(21A)···S(4)[g]	0.97	2.88	3.778(4)	154.4
C(46)−H(46B)···S(1)[h]	0.97	2.76	3.669(4)	156.9
C(49)−H(49B)···S(4)[h]	0.97	2.83	3.780(4)	166.9
C(38)−H(38A)···N(3)[i]	0.97	2.64	3.584(6)	163.6
C(37)−H(37B)···S(2)[j]	0.97	2.65	3.609(4)	169.5
C(31)−H(31B)···S(2)[j]	0.97	2.90	3.785(5)	152.1

[a]Symmetry transformations used to generate equivalent atoms are given in footnotes *b*−*j*. [b]−*x*,*y*,−*z*+1/2. [c]*x*,*y*−1,*z*. [d]*x*,−*y*+1,*z*+1/2. [e]*x*+1/2,*y*−1/2,*z*. [f]*x*,*y*,*z*+1. [g]−*x*+1,−*y*+1,−*z*+1. [h]−*x*+1,−*y*+1,−*z*. [i]*x*,*y*+1,*z*. [j]*x*−1,*y*+1,*z*.

*$[Bu_4N]_2[Ni(Cl_2$6,7-qdt$)_2]$ (**3**).* The crystals of compound **3**, for single crystal X-ray structure determination, were recrystallized from acetonitrile solution by the vapor diffusion of diethyl ether. X-ray crystal structure analysis shows that compound **3** crystallizes in monoclinic space group $P2(1)/c$. The relevant asymmetric unit of the compound **3** contains half a molecule of $[Ni(Cl_2$6,7-qdt$)_2]^{2-}$ anion and one molecule of tetrabutylammonium cation. The thermal ellipsoidal diagram of $[Ni(Cl_2$6,7-qdt$)_2]^{2-}$ anion, present in the compound **3**, is shown in Figure

dx.doi.org/10.1021/ic301017g | Inorg. Chem. 2013, 52, 66−76

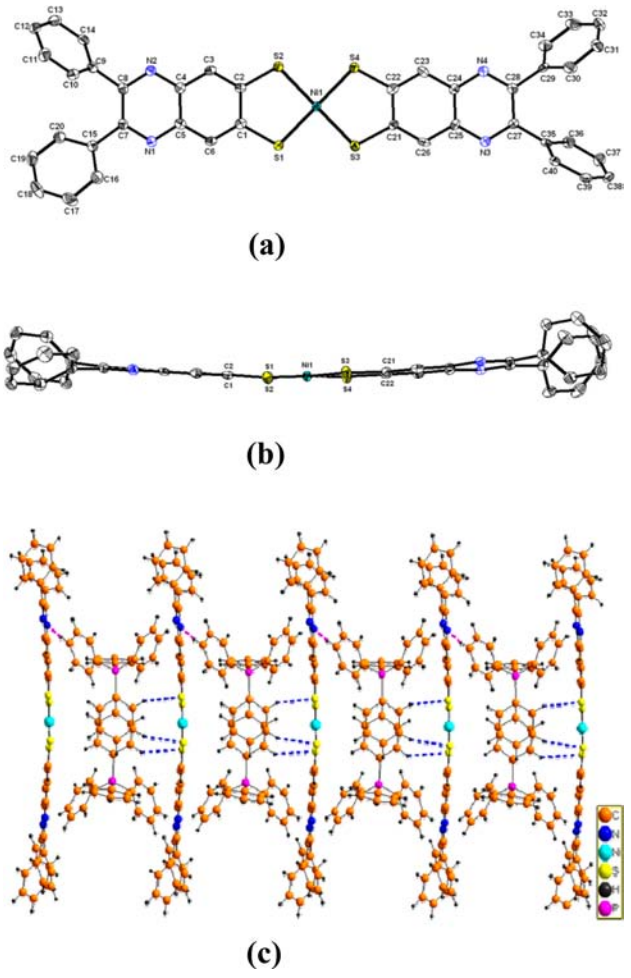

Figure 6. (a) Thermal ellipsoidal diagram of compound **2b** containing complex unit (50% probability); and its (b) sideview representation; (c) one-dimensional supramolecular chain of compound **2b** characterized by C−H···N and C−H···S weak interactions.

7a. Because of the poor quality of the crystal, tetrabutylammonium cation, present in the crystal structure of the compound **3**, suffers from significant disorder as shown in Supporting Information, Figure S6. Because of this, we could not study weak interactions between the cations and the anions in the relevant crystal structure. Although few attempts of recrystallization with various techniques have been made, we could not get a better quality of the single crystals of this compound. In the anion of the compound **3**, the geometry around the Ni^{2+} ion, which is coordinated by four sulfur atoms from two {$Cl_2$6,7-qdt} ligands, shows approximately square planar geometry, because the associated coordination angles are in the range of 88.42(10)°−91.58(10)° which are very close to 90.0° and other coordination angles are 180.0° without any deviation as shown in Figure 7b. However, there is a deviation in the planar nature of the dithiolene-ligand (chelate) present in the compound **3**. The bending deviation (η) between the SMS plane and SCCS plane is characterized by the angle of 5.32° present in the {Ni1S1S2C1C2} chelate in **3**.

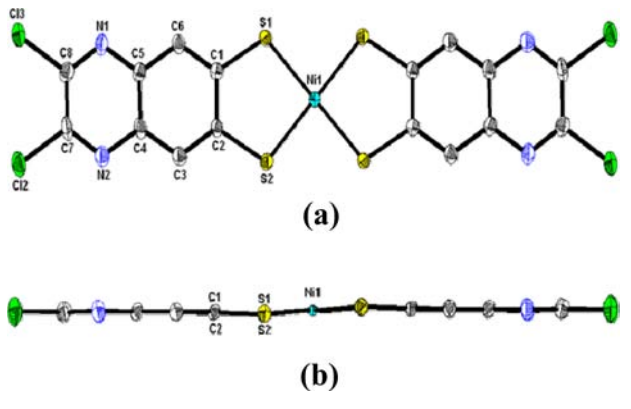

Figure 7. (a) Thermal ellipsoidal diagram of compound **3** containing complexic unit (20% probability); and its (b) side view representation.

*[Bu_4N]$_2$[Ni($Me_2$6,7-qdt)$_2$] (**4**).* The crystals of compound **4**, suitable for single crystal X-ray structure determination, were obtained from acetonitrile solution by the vapor diffusion of diethyl ether. Crystallographic analysis reveals that compound **4** crystallizes in triclinic space group $P\bar{1}$. The relevant asymmetric unit contains one molecule of $[Ni(Me_2$6,7-qdt$)_2]^{2-}$ anion and two molecules of tetrabutylammonium cations. The thermal ellipsoidal plot of $[Ni(Me_2$6,7-qdt$)_2]^{2-}$ anion, present in compound **4**, is shown Figure 8a. In the anion of the compound **4**, the geometry around the Ni^{2+} ion, which is coordinated by four sulfur atoms from two $Me_2$6,7-qdt ligands, shows distortion from square planar geometry; the relevant distortion is between the two SMS planes with a dihedral angle of 4.87°, because the coordination angles are in the range of 175.30(5)°−177.89(5)° and 87.93(4)°−91.22(4)° which are deviated from 180.0° and 90.0°, respectively. The distortion of the {NiS_4} core from square planar geometry is clearly shown in the side view of complex anion in compound **4** (Figure 8b), whereas complexes **1a** and **1b** do not show similar distortion. The reason for this distortion from the square planar geometry (compound **4**) may be due to the involvement of the sulfur atoms in extensive C−H···S hydrogen bonding interactions. The bending deviations (η) between the {S1Ni1S2} and {S1C1C6S2} planes, and {S3Ni1S4} and {S3C11C16S4} planes, are characterized by the angles of 6.24°and 4.53° present in {Ni1S1S2C1C6} and {Ni1S3S4C11C16} dithiolate-chelates, respectively.

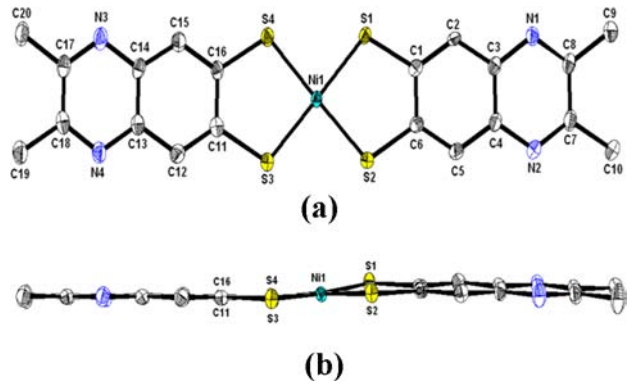

Figure 8. (a)Thermal ellipsoidal diagram of compound **4** containing complex unit (40% probability); and its (b) side view representation.

In the crystal structure of the compound **4**, three out of four sulfur atoms in each dithiolate anionic complex are characterized by six C−H···S hydrogen bonding contacts with four surrounding $[Bu_4N]^+$ cations and one C−H···N hydrogen bonding contact with one $[Bu_4N]^+$ cation as shown the Supporting Information, Figure S7. In the asymmetric unit of

dx.doi.org/10.1021/ic301017g | *Inorg. Chem.* 2013, 52, 66−76

the crystal structure, there are two types of $[Bu_4N]^+$ cations characterized by six C−H···S hydrogen-bond contacts with three surrounding anions and one C−H···N hydrogen-bonding contact with one anion as shown in Figure 9a. The relevant

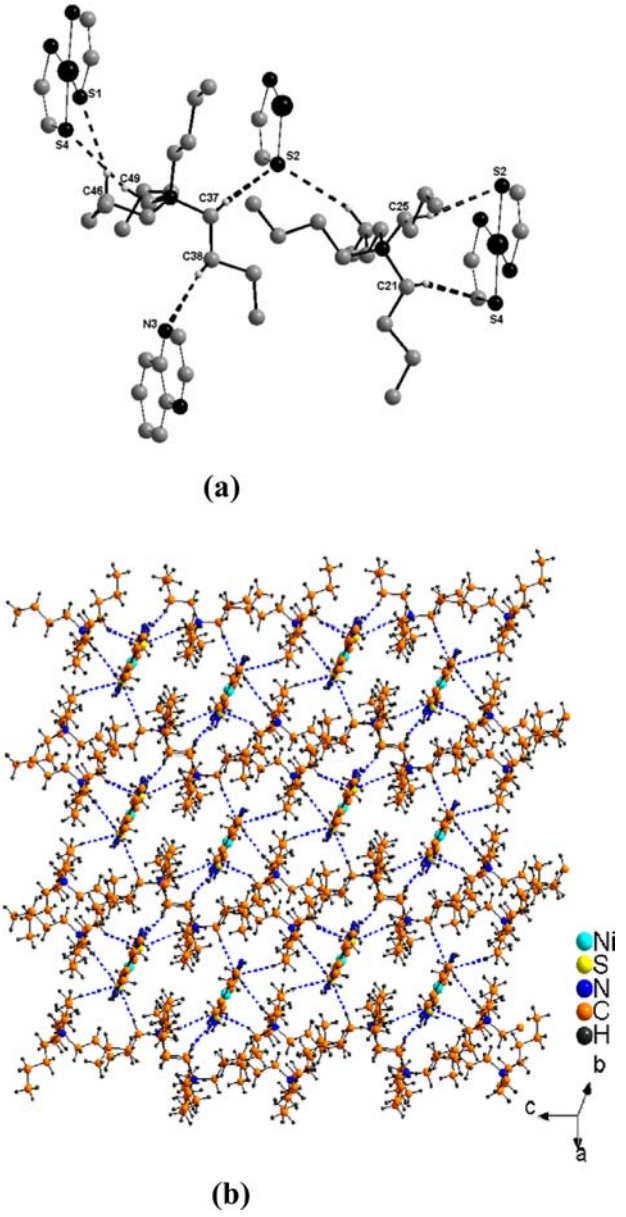

Figure 9. (a) View of the asymmetric unit of compound **4** (thick solid lines) (some of the hydrogen atoms are removed for clarity) showing all the H-bonding intermolecular cation−anion contacts (dotted lines) with other surrounding moieties (thin solid lines); (b) two-dimensional supramolecular network of compound **4** is characterized by C−H···N and C−H···S weak interactions.

hydrogen bonding geometrical parameters are listed in the Table 5. The effective combination of C−H···S and C−H···N weak hydrogen bonding interactions between the cation and the anions result in a two-dimensional supramolecular network as shown in Figure 9b.

CONCLUSIONS

With the aim of designing new quinoxaline dithiolate ligands and their metal coordination complexes, we have synthesized a new series of square-planar nickel-bis(quinoxaline-6,7-dithiolate) complexes with the general formula $[Bu_4N]_2[Ni(X_2$6,7-qdt$)_2]$, where X = H (**1a**), Ph (**2a**), Cl (**3**), and Me (**4**). Solution and solid state electronic absorption spectra of all these compounds show broad bands in the visible region that are due to the CT transitions involving electronic excitation from a HOMO which is a mixture of dithiolate (π) and metal (d) orbital character to a LUMO which is a π^* orbital of the dithiolate. The present ligand system $(6,7\text{-qdt})^{2-}$, in comparison with the existing well-studied ligand $(qdt)^{2-}$, is unique. The change in position of ring nitrogen atoms from sulfur-attached ring to adjacent ring makes a lot of difference in terms of oxidation potential of the resulting coordination complexes, for example, $[Ni(6,7\text{-qdt})_2]^{2-}$ has much lower oxidation potential than that of $[Ni(qdt)_2]^{2-}$. Therefore, the effect of substitution of this new class of ligands on the electronic structures of the relevant metal-coordination complexes is an important approach not only in metal-dithiolene chemistry but also in bioinorganic chemistry (modeling active sites of molybdenum hydroxylases). The active sites of molybdenum hydroxylases contain a similar ligand system, in which the ring nitrogens are not present in the sulfur attached ring but in the adjacent second ring as observed in $(6,7\text{-qdt})^{2-}$. The electrochemical properties (the first oxidation potentials) and the electronic absorption spectral behavior of the present system $[Bu_4N]_2[Ni(X_2$6,7-qdt$)_2]$ (X = H, Ph, Cl, and Me) are dependent on the nature of the electron donating/withdrawing groups (X) attached to the 6,7-quinoxaline dithiolene core moiety. Thus the present study serves to understand the role of substituents of a particular ligand on electron/CT in frontier orbitals. Moreover, the present system has potential to be a good oxidation catalyst as indicated by its low oxidation potential. Presently, we are working on synthesis, characterization, and reactivity of oxo-molybdenum/tungsten complexes with the same ligands with relevance to the active sites of oxo-transferase metalloenzymes.

ASSOCIATED CONTENT

Supporting Information

Crystallographic data in CIF format and computational outputs (coordinates of the G03 optimized structures) for compounds **1a**, **2b**, **3**, and **4**. Further details are given in Figures S1−S21. This material is available free of charge via the Internet at http://pubs.acs.org.

AUTHOR INFORMATION

Corresponding Author

*E-mail: skdsc@uohyd.ernet.in, samar439@gmail.com. Fax: +91-40-2301-2460. Tel: +91-40-2301-1007.

Notes

The authors declare no competing financial interest.

ACKNOWLEDGMENTS

Our special thanks to Professor S. Mahapatra, School of Chemistry, University of Hyderabad, for his help in theoretical calculations. We thank Department of Science and Technology, Government of India, for financial support (Project No. SR/SI/IC-23/2007). The National X-ray Diffractometer facility at University of Hyderabad by the Department of Science and Technology, Government of India, is gratefully acknowledged. We are grateful to UGC, New Delhi, for providing infrastructure facility at University of Hyderabad under a UPE grant.

R.B., S.N.R., and G.D. thank CSIR India for their fellowships, and V.S. thanks UGC networking centre. We also thank the Centre for Nanotechnology, University of Hyderabad, for support. We are grateful to Professor S. Pal and his group for providing us the facility of electrochemical experiments.

DEDICATION

†Dedicated to Professor Sabyasachi Sarkar on the occasion of his 65th birthday.

REFERENCES

(1) Karlin, K. D.; Stiefel, E. I. *Prog. Inorg. Chem.*, John Wiley: New York, 2004; Vol. *52*.

(2) (a) Kato, R. *Chem. Rev.* **2004**, *104*, 5319. (b) Mercuri, M. L.; Deplano, P.; Pilia, L.; Serpe, A.; Artizzu, F. *Coord. Chem. Rev.* **2010**, *254*, 1419. (c) Coomber, A. T.; Beljonne, D.; Friend, R. H.; Brédas, J. L.; Charlton, A.; Robertson, N.; Underhill, A. E.; Kurmoo, M.; Day, P. *Nature* **1996**, *380*, 144. (d) Ren, X. M.; Nishihara, S.; Akutagawa, T.; Noro, S.; Nakamura, T. *Inorg. Chem.* **2006**, *45*, 2229. (e) Robertson, N.; Cronin, L. *Coord. Chem. Rev.* **2002**, *227*, 93.

(3) (a) Deplano, P.; Pilia, L.; Espa, D.; Mercuri, M. L.; Serpe, A. *Coord. Chem. Rev.* **2010**, *254*, 1434. (b) Serrano-Andrés, L.; Avramopoulos, A.; Li, J.; Labéguerie, P.; Bégué, D.; Kellö, V.; Papadopoulos, M. G. *J. Chem. Phys.* **2009**, *131*, 134312. (c) Chen, C.-T.; Liao, S.-Y.; Lin, K.-J.; Lai, L.-L. *Adv. Mater.* **1998**, *3*, 334.

(4) (a) Mueller-Westerhoff, U. T.; Vance, Yoon, B. D. I. *Tetrahedron* **1991**, *47*, 909. (b) Deplano, P.; Mercuri, M. L.; Pintus, G.; Trogu, E. F. *Comments Inorg. Chem.* **2001**, *22*, 353. (c) Bai, J.-F.; Zuo, J.-L.; Tan, W.-L.; Ji, W.; Shen, Z.; Fun, H.-K.; Chinnakali, K.; Razak, I. A.; You, X.-Z.; Che, C.-M. *J. Mater. Chem.* **1999**, *9*, 2419. (d) Aragoni, M. C.; Arca, M.; Cassano, T.; Denotti, C.; Devillanova, F. A.; Frau, R.; Isaia, F.; Lelj, F.; Lippolis, V.; Nitti, L.; Romaniello, P.; Tommasi, R.; Verani, G. *Eur. J. Inorg. Chem.* **2003**, 1939.

(5) (a) Hine, F. J.; Taylor, A. J.; Garner, C. D. *Coord. Chem. Rev.* **2010**, *254*, 1570. (b) Rees, D. C.; Hu, Y.; Kisker, C.; Sahindelin, H. *J. Chem. Soc., Dalton. Trans.* **1997**, 3909. (c) Rudolph, M. J.; Wuebbens, M. M.; Rajagopalan, K. V.; Sahindelin, H. *Nat. Struct. Biol.* **2001**, *8*, 42.

(6) (a) Johnson, J. L.; Rajagopalan, K. V. *Proc. Natl. Acad. Sci. U.S.A.* **1982**, *79*, 6856. (b) Johnson, J. L.; Hainline, B. E.; Rajagopalan, K. V.; Arison, B. H. *J. Biol. Chem.* **1984**, *259*, 5414.

(7) (a) Boyde, S.; Garner, C. D.; Enemark, J. H.; Bruck, M. A.; Kristofzski, J. G. *J. Chem. Soc., Dalton. Trans.* **1987**, 2267. (b) Boyde, S.; Garner, C. D.; Enemark, J. H.; Ortega, R. B. *J. Chem. Soc., Dalton. Trans.* **1987**, 297. (c) Boyde, S.; Garner, C. D.; Enemark, J. H.; Ortega, R. B. *Polyhedron* **1986**, *5*, 377.

(8) Rabaça, S.; Almeida, M. *Coord. Chem. Rev.* **2010**, *254*, 1493.

(9) (a) Kobayashi, Y.; Jacobs, B.; Allendorf, M. D.; Long, J. R. *Chem. Mater.* **2010**, *22*, 4120. (b) Baudron, S. A.; Hosseini, M. W. *Inorg. Chem.* **2006**, *45*, 5260. (c) Ribas, X.; Dias, J. C.; Morgado, J.; Wurst, K.; Molins, E.; Ruiz, E.; Almeida, M.; Veciana, J.; Rovira, C. *Chem.—Eur. J.* **2004**, *10*, 1691. (d) Ribas, X.; Dias, J.; Morgado, J.; Wurst, K.; Almeida, M.; Veciana, J.; Rovira, C. *CrystEngComm* **2002**, *4*, 564. (e) Ribas, X.; Maspoch, D.; Dias, J.; Morgado, J.; Almeida, M.; Wurst, K.; Vaughan, G.; Veciana, J.; Rovira, C. *CrystEngComm* **2004**, *6*, 589. (f) Takaishi, S.; Hosoda, M.; Kajiwara, T.; Miyasaka, H.; Yamashita, M.; Nakanishi, Y.; Kitagawa, Y.; Yamaguchi, K.; Kobayashi, A.; Kitagawa, H. *Inorg. Chem.* **2009**, *48*, 9048. (g) Ribas, X.; Dias, J. C.; Morgado, J.; Wurst, K.; Santos, I. C.; Almeida, M.; Vidal-Gancedo, J.; Veciana, J.; Rovira, C. *Inorg. Chem.* **2004**, *43*, 3631. (h) Dawe, L. N.; Miglioi, J.; Turnbow, L.; Taliaferro, M. L.; Shum, W. W.; Bagnato, J. D.; Zakharov, L. N.; Rheingold, A. L.; Arif, A. M.; Fourmigué, M.; Miller, J. S. *Inorg. Chem.* **2005**, *44*, 7530. (i) Bolligarla, R.; Das, S. K. *CrystEngComm* **2010**, *12*, 3409. (j) Bolligarla, R.; Tripuramallu, B. K.; Sreenivasulu, V.; Das, S. K. *Indian J. Chem. A* **2011**, *50*, 1410.

(10) (a) Kumaki, D.; Tokito, S.; Yamashita, Y. *J. Am. Chem. Soc.* **2006**, *128*, 9598. (b) Nishida, N. J.; Ando, S.; Yamaguchi, J.; Itaka, K.; Koinuma, H.; Tada, H.; Tokito, S.; Yamashita, Y. *J. Am. Chem. Soc.* **2005**, *127*, 10142.

(11) (a) Cummings, S. D.; Eisenberg, R. *Inorg. Chem.* **1995**, *34*, 2007. (b) Cummings, S. D.; Eisenberg, R. *Inorg. Chem.* **1995**, *34*, 3396.

(12) Helton, M. E.; Gebhart, N. L.; Davies, E. S.; McMaster, J.; Garner, C. D.; Kirk., M. L. *J. Am. Chem. Soc.* **2001**, *123*, 10389.

(13) (a) Bolligarla, R.; Kishore, R.; Durgaprasad, G.; Das, S. K. *Inorg. Chim. Acta* **2010**, *363*, 3061. (b) Bolligarla, R.; Durgaprasad, G.; Das, S. K. *Inorg. Chem. Commun.* **2009**, *12*, 355.

(14) Bolligarla, R.; Durgaprasad, G.; Das, S. K. *Inorg. Chem. Commun.* **2011**, *14*, 809.

(15) (a) Baker-Hawkes, M. J.; Billig, E.; Gray, H. B. *J. Am. Chem. Soc.* **1966**, *88*, 4870. (b) Sproulels, S.; Wieghardt, K. *Coord. Chem. Rev.* **2011**, *255*, 837.

(16) Brusso, J. L.; Clements, O. P.; Haddon, R. C.; Itkis, M. E.; Leitch, A. A.; Oakley, R. T.; Reed, R. W.; Richardson, J. F. *J. Am. Chem. Soc.* **2004**, *126*, 8256.

(17) Durgaprasad, G.; Bolligarla, R.; Das, S. K. *J. Organomet. Chem.* **2012**, *706*, 37.

(18) Jia, C.; Liu, S.-X.; Tanner, C.; Leiggener, C.; Neels, A.; Sanguinet, L.; Levillain, E.; Leutwyler, S.; Hauser, A.; Decurtins, S. *Chem.—Eur. J.* **2007**, *13*, 3804.

(19) Bolligarla, R.; Das, S. K. *Tetrahedron Lett.* **2011**, *52*, 2496.

(20) *SADABS, SMART, SAINT, and SHELXTL*; Bruker AXS Inc.: Madison, WI, 2000.

(21) Sheldrick, G. M. *Acta Crystallogr., Sect. A* **2008**, *64*, 112.

(22) Frisch, M. J.; Trucks, G. W.; Schlegel, H. B.; Scuseria, G. E.; Robb, M.; Cheeseman, J. R.; Montgomery, J. A.; Vreven, J. A.; Kudin, K. N.; Burant, J. C.; Millam, J. M.; Iyengar, S. S.; Tomasi, J.; Barone, V.; Mennucci, B.; Cossi, M.; Scalmani, G.; Rega, N.; Petersson, G. A.; Nakatsuji, H.; Hada, M.; Ehara, M.; Toyota, K.; Fukuda, R.; Hasegawa, J.; Ishida, M.; Nakajima, T.; Honda, Y.; Kitao, O.; Nakai, H.; Klene, M.; Li, X.; Knox, J. E.; Hratchian, H. P.; Cross, J. B.; Adamo, C.; Jaramillo, J; Gomperts, R.; Stratmann, R. E.; Yazyev, O.; Austin, A. J.; Cammi, R.; Pomelli, C.; Ochterski, J. W.; Ayala, P. Y.; Morokuma, K.; Voth, G. A.; Salvador, P.; Dannenberg, J. J.; Zakrzewski, V. G.; Dapprich, S.; Daniels, A. D.; Strain, M. C.; Farkas, O.; Malick, D. K.; Rabuck, A. D.; Raghavachari, K.; Foresman, J. B.; Ortiz, J. V.; Cui, Q. ; Baboul, A. G. ; Clifford, S. ; Cioslowski, J.; Stefanov, B. B.; Liu, G.; Liashenko, A.; Piskorz, P.; Komaromi, I.; Martin, R. L.; Fox, D. J.; Keith, T.; Al-Laham, M. A.; Peng, C. Y.; Nanayakkara, A.; Challacombe, M.; Gill, P. M. W.; Johnson, B.; Chen, W.; Wong, M. W.; Gonzalez, C.; Pople, J. A. *Gaussian 03*, Revision B. 05; Gaussian, Inc.: Pittsburgh, PA, 2003.

(23) Becke, A. D. *J. Chem. Phys.* **1993**, *98*, 5648.

(24) Liu, G.; Botting, C. H.; Evans, K. M.; Walton, J. A. G.; Xu, G.; Slawin, A. M. Z.; Westwood, N. J. *ChemMedChem* **2010**, *5*, 41.

(25) (a) Shupack, S. I.; Billig, E.; Clark, R. J. H.; Williams, R.; Gray, H. B. *J. Am. Chem. Soc.* **1964**, *86*, 4594. (b) Schrauzer, G. N.; Mayweg, V. P. *J. Am. Chem. Soc.* **1965**, *87*, 3585. (c) Blomberg, M. R. A.; Wahlgren, U. *Chem. Phys.* **1980**, *49*, 117. (d) Zális, S.; Vlcek, A. A. *Inorg. Chim. Acta* **1982**, *58*, 89. (e) Sano, M.; Adachi., H.; Yamatera, H. *Bull. Chem. Soc. Jpn.* **1981**, *54*, 2636. (f) Clemenson, P. I. *Coord. Chem. Rev.* **1990**, *106*, 171. (g) Guntner, W.; Gliemann, G. *J. Phys. Chem.* **1990**, *94*, 618.

(26) Kirk, M. L.; McNaughton, R. L.; Helton, M. E. *Prog. Inorg. Chem.* **2003**, *52*, 111.

(27) Avilov, I.; Minoofar, P.; Cornil, J.; Cola, L. D. *J. Am. Chem. Soc.* **2007**, *129*, 8247−8258.